

Magnetic Couplings in CsV₂O₅: A New Picture

A. Saúl^{1,*} and G. Radtke²

¹CINaM, UPR 3118 CNRS, Campus de Luminy, case 913, 13288 Marseille cedex 9, France

²IM2NP, UMR 6242 CNRS, Faculté des Sciences de Saint-Jérôme, Case 262, 13397 Marseille cedex 20, France

(Received 7 March 2011; published 29 April 2011)

Concerning its magnetic properties, the layered vanadate CsV₂O₅ has long been considered as formed by isolated spin-1/2 dimers characterized by a large antiferromagnetic coupling of about 146 K. This interpretation was supported by both magnetic susceptibility measurements and the obvious presence of magnetically active strongly dimerized V⁴⁺ ions. In this work we investigate the magnetic properties of this compound through an extensive use of the broken-symmetry formalism in the framework of density-functional theory. Our calculations demonstrate that the system is built from strongly dimerized alternating chains where the structural and magnetic dimers are distinct from each other.

DOI: 10.1103/PhysRevLett.106.177203

PACS numbers: 75.30.Et, 71.20.Lp, 75.10.Dg

The study of low-dimensional spin-1/2 quantum systems has been a very prolific field of condensed matter physics during the past decades. The family of vanadates, in particular, has provided a rich variety of compounds with different behaviors and topologies such as the $\frac{1}{5}$ -depleted quasi-two-dimensional square lattice [1], two-leg ladders [2,3], one-dimensional chains [4,5], or isolated dimers [6,7]. Their magnetic structure and properties are primarily determined by the magnitude and the sign of the different effective exchange couplings arising between magnetic ions and therefore on the very details of their atomic and electronic structures. In this framework, the sole consideration of the geometry of a compound, usually based on a simple analysis of the distances separating the magnetic centers, is often incomplete and even misleading. A detailed experimental investigation of (VO)₂P₂O₇ by inelastic neutron scattering [8] demonstrated, for example, that the magnetic properties of this compound, originally considered as an excellent realization of a two-leg spin ladder, were in fact those of an alternating Heisenberg antiferromagnetic (AFM) chain running perpendicularly to the supposed ladder direction. The determination of exchange couplings is therefore crucial to unravel the complex magnetic behavior of certain compounds but also to guide the design of new systems.

The layered vanadate CsV₂O₅ has long been considered a realization of isolated spin-1/2 dimers system [9] characterized by a large AFM intradimer coupling of about 146 K [6]. This interpretation was based on the good fit of the static magnetic susceptibility and supported by the presence of structurally dimerized magnetic V⁴⁺ ions. This compound indeed crystallizes in a monoclinic structure [10] with space group *P*2₁/*c* where layers of [V₂O₅]⁻ are stacked along the crystallographic axis **a** and separated by layers of Cs ions. There are four chemical units (32 atoms) in the crystallographic unit cell. Two crystallographically inequivalent vanadium sites are present in the layers corresponding, respectively, to nonmagnetic V⁵⁺ in

tetrahedral sites and magnetic V⁴⁺ in square pyramids, as shown in Fig. 1(a). The square pyramids share an edge (through the O₍₅₎ atoms) in such a way that the two apical O₍₃₎ atoms are located above and below the plane formed by the equatorial oxygens. These structural [V₂⁽⁴⁺⁾O₈]⁸⁻ dimers are linked to each other through bridging [V⁽⁵⁺⁾O₄]³⁻ units and form chains oriented along the **c** axis.

In a crude ionic picture, the only atoms having an open shell configuration are the four V⁴⁺ ions, with one electron in the 3*d*_{*y*²-*z*²} orbital. A theoretical study of this compound based on density-functional theory (DFT) calculations and followed by a tight-binding analysis of the paramagnetic vanadium *d*_{*y*²-*z*²} bands pointed out the presence of a significant interdimer interaction along the chains and the impossibility to draw any conclusion about the nature of the system (alternating 1D chains or isolated dimers) based only on the analysis of the static magnetic susceptibility [11]. Recent experiments also pointed out the unrealistic character of the isolated dimer model mentioned previously [7].

In this Letter, we demonstrate, based on first-principles calculations, that the magnetic structure of CsV₂O₅ is made of strongly dimerized alternating 1D chains oriented along the **c** axis. Moreover, we show that the largest exchange coupling along the chain arises unexpectedly *between* the structural dimers, via the V⁴⁺-O-V⁵⁺-O-V⁴⁺ superexchange pathway or, in other words, that the structural dimers are *not* the magnetic dimers.

DFT calculations were carried out by using the full potential linearized augmented plane wave plus local orbitals [FP-(L)APW + lo] method as implemented in the WIEN2K code [12]. The hybrid PBE0 [13] exchange-correlation functional, designed to improve the treatment of strongly correlated electrons within the framework of DFT calculations, has been employed in this work. In this case, a 1/4 fraction of exact (Hartree-Fock) exchange is

substituted to generalized gradient approximation (GGA) semilocal exchange (PBE [14]). This substitution is, however, restricted to the subspace spanned by states of strongly correlated electrons [15,16], i.e., the $V-3d$ states in CsV_2O_5 .

The evaluation of exchange couplings is based on the broken-symmetry formalism [17,18], i.e., the computation of total energies for supercells characterized by different collinear arrangements of the V^{4+} magnetic moments. Let us suppose first that the magnetic excitations in CsV_2O_5 can be described with an Heisenberg Hamiltonian:

$$\hat{H} = \hat{H}_0 + \sum_{i>j} J_{ij} \hat{S}_i \hat{S}_j, \quad (1)$$

where \hat{H}_0 represents the spin-independent part of the Hamiltonian, \hat{S}_i and \hat{S}_j stem for the spin-1/2 operators localized on sites i and j , respectively, and J_{ij} is the magnetic coupling between these moments. A state $|\alpha\rangle$ characterized by a particular collinear spin arrangement of the magnetic moments within the supercell (i.e., $|\alpha\rangle$ is close to an eigenstate of the individual \hat{S}_{iz} operators, such that $\hat{S}_{iz}|\alpha\rangle \simeq \pm \frac{1}{2}|\alpha\rangle$) is obtained by preparing accordingly the initial electronic density and running the self-consistent loop until convergence. It is then easy to show that the expectation value of Hamiltonian (1) on such a state can be simply written under the form of an Ising Hamiltonian [19]:

$$\epsilon_{\alpha}^{\text{DFT}} = \langle \alpha | \hat{H} | \alpha \rangle = \epsilon_0 + \sum_{i>j} \frac{J_{ij}}{4} \sigma_i \sigma_j \quad (2)$$

with $\sigma_i = \pm 1$. Magnetic couplings up to the fourth-nearest neighbor within the V_2O_5 planes, shown in Fig. 1(b), have been evaluated. The first- and third-nearest-neighbor interactions J_1 ($d_{VV} = 3.07 \text{ \AA}$) and J_3 ($d_{VV} = 5.50 \text{ \AA}$) are located along the chains and correspond, respectively, to the interactions arising within the structural dimers and between these dimers. The second- and fourth-nearest-neighbor interactions J_2 ($d_{VV} = 5.39 \text{ \AA}$) and J_4 correspond to interchain interactions, $J_4 = \frac{1}{2}(J'_4 + J''_4)$ being evaluated as the average value of interactions J'_4 ($d_{VV} = 5.95 \text{ \AA}$) and J''_4 ($d_{VV} = 6.65 \text{ \AA}$) shown in Fig. 1(b). This latter approximation is justified both by the similarities in the superexchange pathways associated to J'_4 and J''_4 and by the fact that these interactions are expected to be relatively weak due to the correspondingly large $V^{4+}-V^{4+}$ interatomic distances. One might therefore express energies (2) in terms of these couplings as

$$\epsilon_{\alpha}^{\text{DFT}} = \epsilon_0 + \sum_{k=1}^4 a_{\alpha k} J_k, \quad (3)$$

where the coefficients $a_{\alpha k}$ depend on the configuration under consideration. In order to calculate these four magnetic couplings, 64-atom supercells obtained by doubling the monoclinic unit cell along the \mathbf{c} axis and containing eight magnetic ions were used. A total of $2^8 = 256$ possible configurations are therefore obtained with this

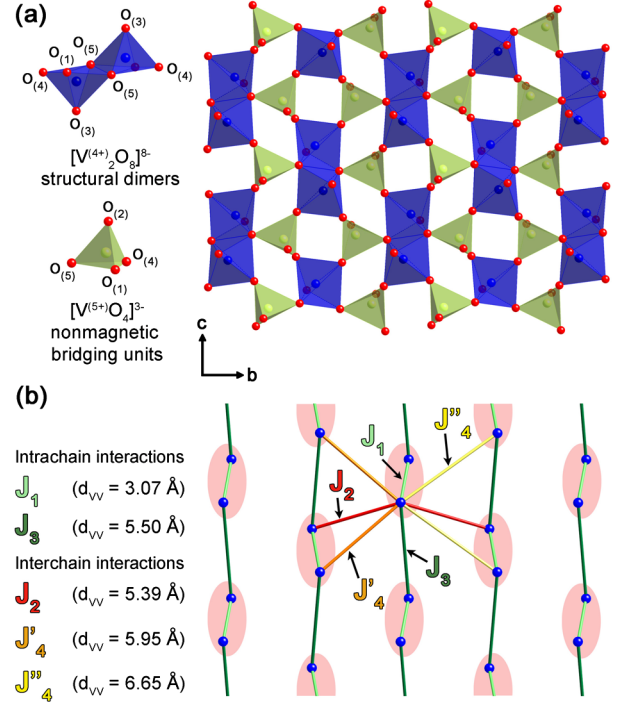


FIG. 1 (color online). (a) Structure of the $[\text{V}_2\text{O}_5]^-$ layers in CsV_2O_5 . The blue and light green balls denote, respectively, the magnetic V^{4+} and the nonmagnetic V^{5+} ions, and the red balls denote the O ions. (b) Network of the magnetic interaction between V^{4+} ions in the structure. Shaded regions emphasize structural dimers.

choice of supercell. Spin reversal and crystalline symmetries reduce this number to 28 inequivalent configurations of respective degeneracies g_{α} .

Magnetic couplings were finally obtained through a least-squares fit procedure [17], i.e., by minimization of

$$F = \sum_{\alpha=1}^{28} g_{\alpha} \left(\epsilon_{\alpha}^{\text{DFT}} - \epsilon_0 - \sum_{k=1}^4 a_{\alpha k} J_k \right)^2. \quad (4)$$

The results of this minimization procedure are illustrated in Fig. 2. The dominant interactions in this compound are AFM and located along the dimer chains, i.e., along the \mathbf{c} axis of the crystal. Unexpectedly, the interaction $J_3 = 188 \text{ K}$ involving a superexchange pathway through the covalently bonded $V^{(5+)}\text{O}_4$ bridging groups between the dimers is predicted to be more than twice as large as the intradimer interaction $J_1 = 89 \text{ K}$, revealing that the magnetic dimers along the chain are not the structural ones. The remaining interchain interactions are much weaker and ferromagnetic: $J_2 = -23 \text{ K}$ and $J_4 = -3 \text{ K}$. The magnetic structure of CsV_2O_5 suggested by these calculations is therefore closer to an alternating 1D chain than to the isolated dimer picture originally drawn for this compound. It should be noted here that the small standard deviation $\sigma = 4 \text{ K}$ obtained by using this procedure confirms the appropriateness of interpreting DFT energy differences with an Heisenberg spin Hamiltonian.

Complementary calculations were performed to verify the relevance of these results. First, magnetic couplings computed with the GGA-PBE semilocal exchange-correlation functional deliver the same overall picture as the PBE0 functional, predicting the same signs and ratios between the different interactions. However, the GGA shows a clear tendency to overestimate the amplitudes of these interactions by a factor of ~ 2 with respect to PBE0. This well known failure of local and semilocal exchange-correlation functionals to describe localized states and leading to an overestimation of the amplitude of magnetic couplings [20] is partly overcome in PBE0, predicting interactions of the same order of magnitude as estimated from experiments [6,7,9]. Second, calculations performed on 64-atom supercells doubling the monoclinic unit cell along the \mathbf{a} axis confirmed the absence of interplane interaction occurring via the Cs layers. Finally, a full structural optimization of the monoclinic cell has also been performed by using the PBE0 functional. Equilibrium lattice parameters $a = 7.46 \text{ \AA}$, $b = 9.95 \text{ \AA}$, $c = 7.88 \text{ \AA}$, and $\gamma = 90.65^\circ$ slightly overestimate their experimental values in the covalent plane ($\sim 1\%$), as expected for a GGA based exchange-correlation functional. The a parameter, related to the interplane separation, is about 6% larger than the experimental one. The magnetic couplings calculated with this relaxed structure are similar to those obtained with the experimental structure.

This surprising result ($J_3 > J_1$) can be understood qualitatively by visualizing the spatial distribution of the electron density associated with the magnetic orbital centered on a V^{4+} ion. To this end, we selected the only broken-symmetry configuration containing one, and only one, flipped spin V^{4+} ion in the supercell (spin down), the remaining seven V^{4+} ions holding an antiparallel (spin up) magnetic moment. The use of a 64-atom supercell ensures here a sufficient spatial separation between this

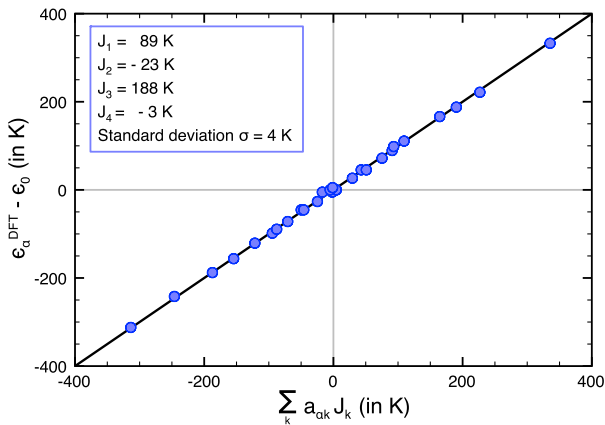


FIG. 2 (color online). Graphical representation of the results obtained by using the least-squares fit procedure: For each configuration, the DFT relative energy $e_\alpha^{\text{DFT}} - \epsilon_0$ is represented as a function of the optimized Ising energy. The best fit values are shown in the inset. According to the convention used in Eq. (1), positive couplings correspond to AFM interactions.

ion and its periodically repeated image within the V_2O_5 planes ($\sim 9.90 \text{ \AA}$) leading to the formation of a corresponding dispersionless minority spin band. The electron density associated with this “broken-symmetry magnetic orbital” is displayed in Fig. 3.

The weak amplitude of the first-nearest-neighbor interaction J_1 can be understood by considering the dominant $V^{4+} - d_{y^2-z^2}$ character of the orbitals involved in the intradimer superexchange interaction. The symmetry of these orbitals indeed greatly hinders the close to 90° V-O-V superexchange interaction [21] occurring via the $O_{(5)}$ atoms located in the equatorial plane of the structural dimers (see Fig. 3). Interestingly, a delocalization of the magnetic orbital toward the nonmagnetic VO_4 tetrahedra is also observed in Fig. 3 through its nonzero components on both $O_{(1)}$ and $O_{(4)}$ p orbitals and on a low crystal field energy $V^{5+} d$ orbital (approximately located in the plane perpendicular to the shortest V-O bond of the tetrahedron). This delocalization opens the way to the large interdimer interaction J_3 , mediated by the tetrahedral VO_4 bridging units.

To further investigate this point, we have correlated the strength of the AFM contributions to the magnetic couplings derived from a one-band Hubbard model $J^{\text{AFM}} \approx 4t^2/U$ (where U is the effective on-site Coulomb repulsion) with the ones (J_1 and J_3) obtained by total energy differences. We analyzed the $V^{4+} - d_{y^2-z^2}$ bands by using a tight-binding model including hopping terms up to the fourth-nearest neighbors (t_1, t_2, t_3 , and t_4) and defined in a similar manner as the exchange integrals shown in Fig. 1(b) [22]. The spin projected band structure for a ferromagnetic PBE0 calculation is shown in Fig. 4.

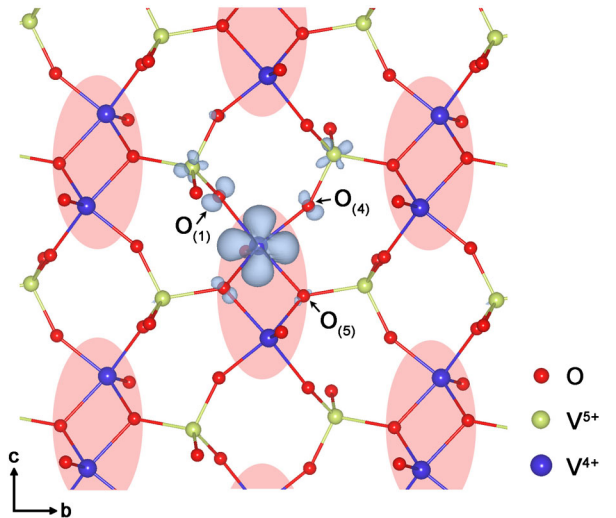


FIG. 3 (color online). Minority spin electron density corresponding to a calculation with only one spin down V^{4+} ion in the supercell, the remaining seven V^{4+} holding a spin up magnetic moment. The isosurface corresponding to a density of 4.10^{-3} electron a.u. $^{-3}$ is shown. Shaded regions emphasize structural dimers.

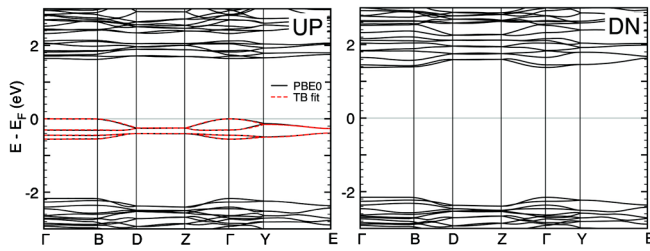


FIG. 4 (color online). Spin projected band structure calculated for a ferromagnetic arrangement of the four V^{4+} magnetic moments in the CsV_2O_5 crystallographic unit cell. The dashed (red) curves correspond to the tight-binding fit of the spin up PBE0 $d_{y^2-z^2}$ bands.

The four $d_{y^2-z^2}$ bands can be clearly distinguished in the spin up band structure plot just below the Fermi energy. The corresponding bands obtained from a tight-binding Hamiltonian with effective hopping integrals $t_3 = 117 > t_1 = 55 > t_2 = 25 \sim t_4 = 26$ meV are also shown. Despite its excellent agreement with the DFT bands, this ferromagnetic model is unable to lift an intrinsic ambiguity related to the symmetry of the problem. It is indeed possible to define a unitary transformation U , permuting the role played by the hopping integrals t_1 and t_3 along the chains, i.e., $H'(t_3, t_2, t_1, t_4) = U^{-1}H(t_1, t_2, t_3, t_4)U$, such that a fit cannot be used to distinguish these two parameters.

A straightforward extraction of these hopping parameters is, however, made possible by using the broken-symmetry formalism. The intradimer t_1 parameter can indeed be extracted from the minority spin bands of a calculation performed in a supercell with the two V^{4+} ions of the same dimer having a spin down and the remaining six V^{4+} in a spin up configuration [see Fig. 5(b)]. In the same manner, the interdimer hopping integral t_3 can be estimated by using a supercell with two spin down V^{4+} ions facing each other in different dimers as shown in Fig. 5(d). A simple inspection of the respective spin

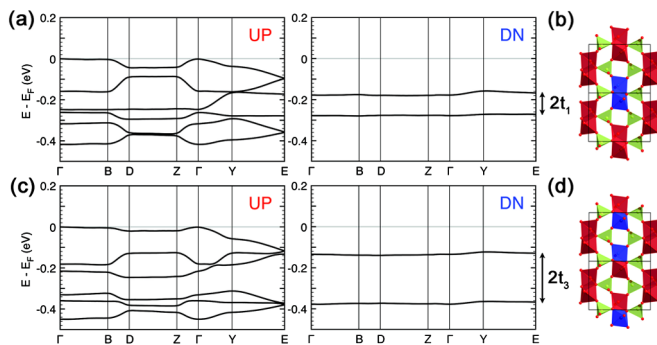


FIG. 5 (color online). (a) Spin projected band structure of the CsV_2O_5 supercell shown in (b) used to estimate the intradimer hopping integral t_1 . (c) Band structure of the broken-symmetry configuration shown in (d) used to estimate the interdimer hopping t_3 . Red and blue square pyramids correspond, respectively, to spin up and down V^{4+} ions.

down band structures [Figs. 5(a) and 5(c)] allows us to unambiguously obtain $t_3 \approx 121 > t_1 \approx 50$ meV, confirming qualitatively the picture obtained previously by total energy differences.

Through an extensive use of the broken-symmetry formalism in DFT, we propose a new picture of CsV_2O_5 where structural and magnetic dimers are distinct from each other. More generally, we demonstrated that nonmagnetic bridging units, such as $[V^{(5+)}O_4]^{3-}$ tetrahedra, play a preponderant role in mediating strong and long ranged AFM interactions in low-dimensional vanadate systems. This theoretical result echoes the experimental work published on $(VO)_2P_2O_7$ [8], where the leading AFM interaction was found to occur through $[P^{(5+)}O_4]^{3-}$ units. This work should motivate further experimental investigations on this compound while emphasizing the importance of nonmagnetic bridging units in the design and the understanding of new systems.

We acknowledge J.-M. Mouesca for his help on the methodological aspects of this work and J. Kohanoff and A. Levy-Yeyati for careful reading of the manuscript.

*saul@cinam.univ-mrs.fr

- [1] S. Tanigushi *et al.*, *J. Phys. Soc. Jpn.* **64**, 2758 (1995).
- [2] H. Iwase *et al.*, *J. Phys. Soc. Jpn.* **65**, 2397 (1996).
- [3] M. Isobe *et al.*, *J. Phys. Soc. Jpn.* **67**, 755 (1998).
- [4] A. A. Tsirlin, R. Nath, C. Geibel, and H. Rosner, *Phys. Rev. B* **77**, 104436 (2008).
- [5] T. Waki *et al.*, *J. Phys. Soc. Jpn.* **73**, 3435 (2004).
- [6] M. Isobe and Y. Ueda, *J. Phys. Soc. Jpn.* **65**, 3142 (1996).
- [7] I. S. Camara *et al.*, *Phys. Rev. B* **81**, 184433 (2010).
- [8] A. W. Garrett *et al.*, *Phys. Rev. Lett.* **79**, 745 (1997).
- [9] J. Mur and J. Darriet, *C.R. Acad. Sci. Ser. Gen., Ser. 2* **300**, 599 (1985).
- [10] K. Walthersson and B. Forslund, *Acta Crystallogr. B* **33**, 789 (1977).
- [11] R. Valentí and T. Saha-Dasgupta, *Phys. Rev. B* **65**, 144445 (2002).
- [12] P. Blaha, K. Schwarz, G. Madsen, D. Kvaniscka, and J. Luitz, in *WIEN2K, An Augmented Plane Wave + Local Orbitals Program for Calculating Crystal Properties*, edited by K. Schwarz (Technische Universtat Wien, Austria, 2001).
- [13] M. Ernzerhof and G. Scuseria, *J. Chem. Phys.* **110**, 5029 (1999).
- [14] J. Perdew, K. Burke, and M. Ernzerhof, *Phys. Rev. Lett.* **77**, 3865 (1996).
- [15] P. Novák *et al.*, *Phys. Status Solidi B* **243**, 563 (2006).
- [16] F. Tran *et al.*, *Phys. Rev. B* **74**, 155108 (2006).
- [17] L. Li *et al.*, *Inorg. Chem.* **45**, 7665 (2006).
- [18] J. M. Mouesca, *J. Chem. Phys.* **113**, 10505 (2000).
- [19] G. Radtke, A. Saúl, H. A. Dabkowska, G. M. Luke, G. A. Botton, *Phys. Rev. Lett.* **105**, 036401 (2010).
- [20] R. L. Martin and F. Illas, *Phys. Rev. Lett.* **79**, 1539 (1997).
- [21] W. E. Pickett, *Phys. Rev. Lett.* **79**, 1746 (1997).
- [22] We define here only one hopping integral $t_4 = t'_4 = t''_4$.